Polymer Chemistry

PAPER

View Article Online
View Journal | View Issue

Cite this: *Polym. Chem.*, 2014, **5**, 1674

PEG-pHPMAm-based polymeric micelles loaded with doxorubicin-prodrugs in combination antitumor therapy with oncolytic vaccinia viruses†

Eduardo Ruiz-Hernández,‡[a] Michael Hess,‡[b] Gustavo J. Melen,[c] Benjamin Theek,[d] Marina Talelli,[ae] Yang Shi,[a] Burcin Ozbakir,[a] Erik A. Teunissen,[a] Manuel Ramírez,[c] Diana Moeckel,[d] Fabian Kiessling,[d] Gert Storm,[f] Hans W. Scheeren,[g] Wim E. Hennink,[a] Aladar A. Szalay,[bhi] Jochen Stritzker*[bh] and Twan Lammers*[adf]

Received 14th August 2013
Accepted 1st October 2013

DOI: 10.1039/c3py01097j

www.rsc.org/polymers

An enzymatically activatable prodrug of doxorubicin was covalently coupled, using click-chemistry, to the hydrophobic core of poly(ethylene glycol)-*b*-poly[*N*-(2-hydroxypropyl)-methacrylamide-lactate] micelles. The release and cytotoxic activity of the prodrug was evaluated *in vitro* in A549 non-small-cell lung cancer cells after adding β-glucuronidase, an enzyme which is present intracellularly in lysosomes and extracellularly in necrotic areas of tumor lesions. The prodrug-containing micelles alone and in combination with standard and β-glucuronidase-producing oncolytic vaccinia viruses were also evaluated *in vivo*, in mice bearing A549 xenograft tumors. When combined with the oncolytic viruses, the micelles completely blocked tumor growth. Moreover, a significantly better antitumor efficacy as compared to virus treatment alone was observed when β-glucuronidase virus treated tumor-bearing mice received the prodrug-containing micelles. These findings show that combining tumor-targeted drug delivery systems with oncolytic vaccinia viruses holds potential for improving anticancer therapy.

Introduction

The administration of anticancer agents is generally associated with dose-limiting side effects. Many different drug delivery systems have been proposed to enhance the biodistribution and the tumor accumulation of chemotherapeutic drugs, and to thereby improve the balance between their efficacy and their toxicity.[1–8] In recent years, polymeric micelles based on poly(ethylene glycol)-*b*-poly[*N*-(2-hydroxypropyl)-methacrylamide-lactate] (mPEG-*b*-pHPMAmLac$_n$) have been investigated as biodegradable carriers of hydrophobic drugs, and have shown significant potential.[9–14]

Doxorubicin (DOX) is a potent anticancer drug and commonly used as a model chemotherapeutic. However, its use is limited by severe cardiotoxicity.[15] For this reason, prodrug therapies have been proposed to increase the therapeutic index of DOX. We recently reported the covalent coupling of a synthetic derivative, DOX-propGA3, to the azide-modified core of mPEG-*b*-pHPMAmLac$_2$ (mPEG-*b*-p(HPMAmLac$_2$-*co*-AzEMA)) micelles.[16] This prodrug showed much less toxicity as compared to the parent drug before two-step activation by (1) chemical hydrolysis of the propargylic ester and (2) conversion to DOX by the enzyme β-glucuronidase. This enzyme is normally present in the lysosomes of (cancer) cells and is released into the extracellular compartment of tumors upon necrosis.[17–20]

Oncolytic virotherapy is a re-emerging therapeutic concept that takes advantage of the tumor-specific replication of viruses. Among the different viruses tested thus far, genetically engineered vaccinia virus strains are among the most promising candidates.[21,22] These viruses display high infectivity and a fast replication cycle, and lead to cell lysis, immune-mediated cell death and vascular collapse within the tumor.[23] In a number of studies, it was shown that recombinant vaccinia viruses (rVACV) derived from the Lister-strain are effective in treating different

[a]*Department of Pharmaceutics, Utrecht Institute for Pharmaceutical Sciences, Utrecht University, Utrecht, The Netherlands. E-mail: tlammers@ukaachen.de; js@genelux.com*
[b]*Department of Biochemistry, Biocenter, University of Würzburg, 97074 Würzburg, Germany*
[c]*Department of Hematooncology & Stem Cell Transplantation Hospital Infantil Universitario Niño Jesús, Madrid, Spain*
[d]*Department of Experimental Molecular Imaging, University Clinic and Helmholtz Center for Biomedical Engineering, Aachen, Germany*
[e]*Department of Inorganic and Bioinorganic Chemistry, Facultad de Farmacia, Universidad Complutense de Madrid, Spain*
[f]*Department of Controlled Drug Delivery, Targeted Therapeutics Section, University of Twente and MIRA Institute for Biomedical Engineering and Technical Medicine, Enschede, The Netherlands*
[g]*Department of Organic Chemistry, Radboud Univ. Nijmegen, Heyendaalseweg 135, 6525 AJ Nijmegen, The Netherlands*
[h]*Genelux Corporation, San Diego Science Center, San Diego, CA 92109, USA*
[i]*Department of Radiation Oncology, Moores Cancer Center, University of California San Diego, La Jolla, CA 92093, USA*

† Electronic supplementary information (ESI) available. See DOI: 10.1039/c3py01097j

‡ These authors contributed equally.

solid tumor types (reviewed in ref. 21). Monitoring of the successful tumor colonization and the therapeutic effects can be performed by different imaging modalities, including optical,[24] optoacoustic,[25] PET-,[26,27] and by MR-imaging.[25] Reporter gene-encoding rVACV can therefore be considered theranostic agents.[28–30]

In addition, vaccinia virus-mediated oncolytic therapy has been combined with radiotherapy[31,32] as well as with chemotherapy.[33] Moreover, the therapeutic effect can be enhanced by vaccinia virus-mediated expression of *e.g.* anti-angiogenic single-chain antibodies[34] or of prodrug-converting enzymes for so-called gene-directed enzyme prodrug therapy (GDEPT).[35] GDEPT and ADEPT (antibody-directed enzyme prodrug therapy) have shown enhanced antitumor efficacy in experimental tumor models in combination with glucuronide prodrugs.[36]

Here, we evaluated the performance of doxorubicin-prodrug-loaded mPEG-*b*-p(HPMAmLac$_2$-*co*-AzEMA) micelles (pg-micelles) against A549 human non-small-cell lung adeno-carcinoma cells (NSCLC) *in vitro* and *in vivo*. The antitumor efficacy of pg-micelles *versus* free DOX was investigated in combination with oncolytic vaccinia virotherapy. Additionally, the influence of virus-encoded overexpression of bacterial β-glucuronidase on the conversion of the prodrug was assessed.

Materials and methods

Synthesis of DOX-propGA3-containing mPEG-*b*-p(HPMAmLac$_2$-*co*-AzEMA) copolymers

The synthesis of the azide-modified copolymer and its covalent linkage to DOX-propGA3 *via* click-chemistry were performed as in ref. 16. In the present study, 80 mol% HPMAmLac$_2$ and 20 mol% AzEMA were polymerized using (mPEG$_{5000}$)$_2$-ABCPA as macroinitiator. For the coupling of the prodrug, DOX-propGA3 and the polymer (5% w/w ratio of DOX-propGA3 to polymer) were dissolved in dimethylformamide. Next, $CuSO_4$ (1 eq. to DOX-propGA3) and sodium ascorbate (1 eq. to DOX-propGA3) dissolved in H_2O were added, and the mixture was stirred for 48 h under a nitrogen atmosphere. The resulting prodrug conjugate was isolated by precipitation in diethyl ether, dissolved in H_2O, dialyzed (membrane cut-off 12–14 kDa) against water for 24 h, and finally recovered by freeze-drying.

Preparation and characterization of pg-micelles

The lyophilized prodrug copolymer conjugate (29 μg DOX-equivalents per mg) was dissolved in PBS (25 mg mL^{-1}) overnight at 0 °C on an orbital shaker. The solution was then incubated in pre-heated (50 °C) water for 60 s to induce the formation of micelles,[37] and subsequently cooled down to room temperature.

Dynamic light scattering (DLS) measurements were performed using a Malvern CGS-3 multiangle goniometer (Malvern Ltd., Malvern, UK, with a JDS Uniphase 22 mW He–Ne laser operating at 632 nm, an optical fiber-based detector and a digital LV/LSE-5003 generator, measurement angle 90°). The autocorrelation function was analyzed by the cumulants method (fitting a single exponential to the correlation function to obtain the mean size and PDI) and the CONTIN routine (fitting a multiple exponential to the correlation function to obtain the distribution of particle size). Transmission electron microscopy (TEM) was carried out on the prodrug-loaded micelles using a Philips Tecnai 12 microscope equipped with a Biotwin-lens and a LaB_6 filament, operated at 120 kV acceleration voltage. Negative uranyl acetate staining (2%) and glow discharged grids (copper 200 mesh grid with a carbon-coated thin polymer film, Formvar on top) were used for sample preparation. Images were captured with a SIS Megaview II CCD-camera and processed with AnalySIS software.

DOX release from pg-micelles (in PBS, pH 7.4, also containing 0.1% w/v bovine serum albumin, at 37 °C) was monitored in the presence and absence of 20 μg mL^{-1} β-glucuronidase (from bovine liver, type B-10, 10 000 units per mg, Sigma-Aldrich Co., Germany). The concentration of DOX-GA3 and DOX in the release medium was measured over time with gradient HPLC, using a C18 Sunfire column and potassium phosphate buffer pH 3 (20 mM) with 5% acetonitrile as eluent A (75–60% in 12 minutes) and 100% acetonitrile as eluent B (excitation wavelength 480 nm, emission wavelength 560 nm).

In vitro cytotoxicity assay

A549 NSCLC were seeded at 5000 cells per cm^2 in DMEM (4.5 g L^{-1} glucose), 100 U mL^{-1} penicillin G, 100 U mL^{-1} streptomycin, 10% fetal bovine serum (FBS) and incubated at 37 °C, 5% CO_2. Cells were exposed to DOX, liposomal DOX (DPPC : cholesterol : DSPE-PEG$_{2000}$ molar composition 1.85 : 1 : 0.15, with comparable characteristics to commercial formulation Doxil®), pg-micelles or empty micelles at serial dilutions ranging from 0.001 to 250 μg mL^{-1} (DOX-equivalents). Cells were incubated with the micellar dispersions with or without the addition of 20 μg mL^{-1} β-glucuronidase. For the *in vitro* cytotoxicity assays, cells were harvested after 3 days and cell viability was determined by flow cytometry with 7AAD (Biolegends, San Diego, CA) using the FACSCanto II flow cytometer and the FACSDiva software v6.1.2 (BD Biosciences, San Jose, CA).

Recombinant vaccinia virus strains

The glucuronidase encoding rVACV GLV-1h68 has been described previously[38] as well as the glucuronidase-negative control rVACV GLV-1h190[39] which encodes TurboFP635 instead of the glucuronidase gene.

Animal experiments

Male athymic nude mice (Harlan, Livermore, CA, USA) were subcutaneously injected on their right flank with 5 × 10^6 A549 cells 30 days (day-30) before DOX or pg-micelles were administered. Fifteen days later (day-15), mice were injected into the retroorbital sinus vein with PBS or 5 × 10^6 pfu of GLV-1h190 and GLV-1h68, respectively. On day 0, mice received injections of PBS (controls), DOX or pg-micelles as treatment, which were repeated on days 5, 10, 16 and 23. For each treatment, 3 mg kg^{-1} DOX-equivalents (free DOX or pg-micelles) were intravenously injected into the lateral tail vein, up to DOX maximum tolerated dose (5 × 3 mg kg^{-1}).[10] Tumor volumes were calculated from

digital caliper measurements (0.5 × length × width^2) and normalized to those on the last day prior to DOX injection. All animal experiments were carried out in compliance with the guidelines of the Institutional Animal Care and Use Committee (IACUC) of Explora BIOLABS (protocol number EB11-025).

Glucuronidase assay

Determination of glucuronidase activity was performed with minor variations according to Hess *et al.*[40] Briefly, tumors were isolated 26 days after the first DOX treatment, weighted, snap-frozen in liquid nitrogen and stored at −80 °C. For the glucuronidase assay, tumors were thawed and lysed in saline (2 mL g^{-1} tumor tissue) using gentleMACS M Tubes (Miltenyi Biotec, Bergisch-Gladbach, Germany) in a gentleMACS dissociator (Miltenyi Biotec). In black 384-well plates with a clear bottom, 5 μL of the lysate was analyzed in a total assay volume of 80 μL containing 2.5 μg fluorescein di-β-D-glucuronide (FDGlcU). The analysis was performed in PBS (pH 7.4) and in acetate buffer (1 M ammonium acetate and 1.2 M acetic acid in dH_2O; pH 4.5) respectively, each supplemented with 2% FBS. After 1 h incubation at 37 °C, the fluorescence signal was read using an Infinite 200 Pro Microplate Reader (Tecan, Crailsheim, Germany; excitation wavelength: 489 nm with 9 nm bandwidth, emission wavelength: 520 nm with 20 nm bandwidth, gain: 75). The results are shown as relative fluorescent units (RFU).

Statistical analysis

Results are presented as average ± standard deviation. Statistical analysis was performed using GraphPad Prism 5.01, employing the two-tailed Student's *t*-test. A *p*-value <0.05 was considered to represent statistical significance.

Results and discussion

The block copolymer mPEG-*b*-p(HPMAmLac$_2$-*co*-AzEMA) was synthesized by free radical polymerization of the HPMAmLac$_2$ and AzEMA monomers with a PEG-based macroinitiator.[16] The molar feed ratio of HPMAmLac$_2$ and AzEMA was 80 : 20, and in the obtained copolymer the ratio was 92 : 8, as calculated from the ^{1}H-NMR spectrum shown in Fig. 1. Thus, 40 mol% of the AzEMA monomer in the feed was built in the polymer.

The azide-modified polymer was reacted with DOX-propGA3[41] by click-chemistry following a Cu(I)-catalyzed azide–alkyne cycloaddition,[42] as schematized in Fig. 2. The molecular weights, M_w (27.0 kDa) and M_n (12.5 kDa), were determined by GPC,[43] giving rise to a polydispersity index (M_w/M_n) of 2.2. A high percentage of prodrug conjugation (90%) was obtained for an azide/DOX-propGA3 molar ratio of 3.9 : 1.

The prodrug-conjugated polymer was soluble in water at 0 °C and had a critical micelle temperature (CMT) of 2 °C.[43] Above the CMT, the thermosensitive block of the polymer, p(HPMAmLac$_2$-*co*-AzEMA), becomes hydrophobic and consequently micelles are formed upon rapid heating to 50 °C. Fig. 3A depicts the reversible formation of micelles with the prodrug localized within the hydrophobic core. The spherical morphology of the micelles was visualized by TEM (Fig. 3B), and

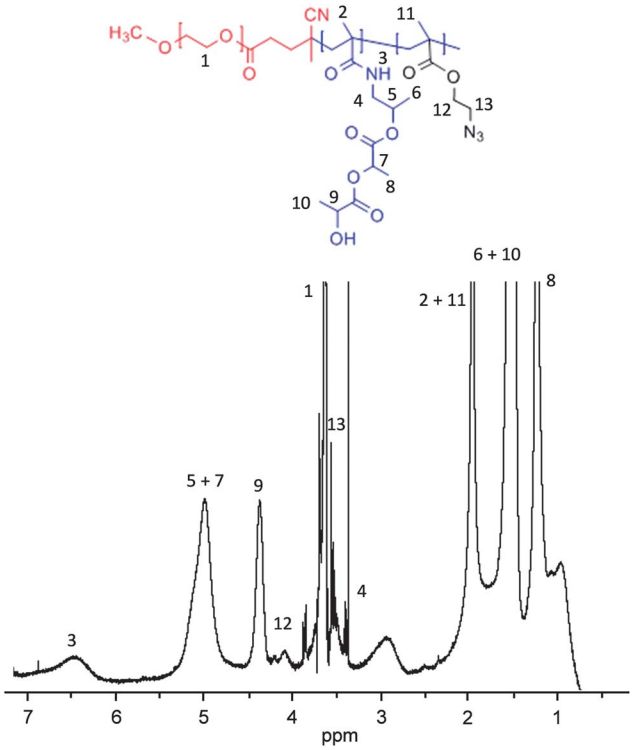

Fig. 1 ^{1}H-NMR spectrum of mPEG-*b*-p(80% HPMAmLac$_2$-*co*-20% AzEMA) in $CDCl_3$.

their hydrodynamic diameter (Z_{avg}: 51 nm) and polydispersity (PDI: 0.064) were determined using DLS (Fig. 3C).

According to the scheme depicted in Fig. 4A, DOX-propGA3 is firstly hydrolyzed and released from the core of the micelles or from (free) polymer chains as an intermediate prodrug of DOX, DOX-GA3. This compound is a substrate for β-glucuronidase, which converts it into free DOX after the cleavage of the glucuronide spacer.[44] Consequently, in the absence of enzyme, only DOX-GA3 is progressively released from the micelles (as detected by HPLC; Fig. 4B), and hardly any conversion of DOX-GA3 to free DOX takes place. When the same experiment is performed in the presence of glucuronidase (20 μg mL^{-1}), DOX-GA3 is rapidly and efficiently converted into free DOX (Fig. 4C). The very similar prodrug release (Fig. 4B) and conversion kinetics (Fig. 4C) show that DOX-GA3 release from the micelles *via* hydrolysis, rather than DOX generation *via* enzymatic cleavage, is the rate-limiting step in drug activation in the presence of enzyme.

The cytotoxicity of pg-micelles was tested in A549 cells (Fig. 5). Empty micelles, with and without the addition of β-glucuronidase in the culture medium, did not affect cell viability in the concentration range tested (0.034–8.600 μg polymer per mL). The prodrug-loaded micelles (0.001 to 250 μg mL^{-1} DOX-equivalents), on the other hand, displayed significant cytotoxicity, in particular in the presence of β-glucuronidase (6-fold higher cytotoxicity as compared to the absence of enzyme: IC_{50} 6.5 *vs.* 1.1 μg DOX-equivalents per mL, respectively; *versus* 0.2 μg per mL for free DOX). The IC_{50} of liposomal DOX (6.7 μg mL^{-1}) was comparable to that of prodrug-loaded

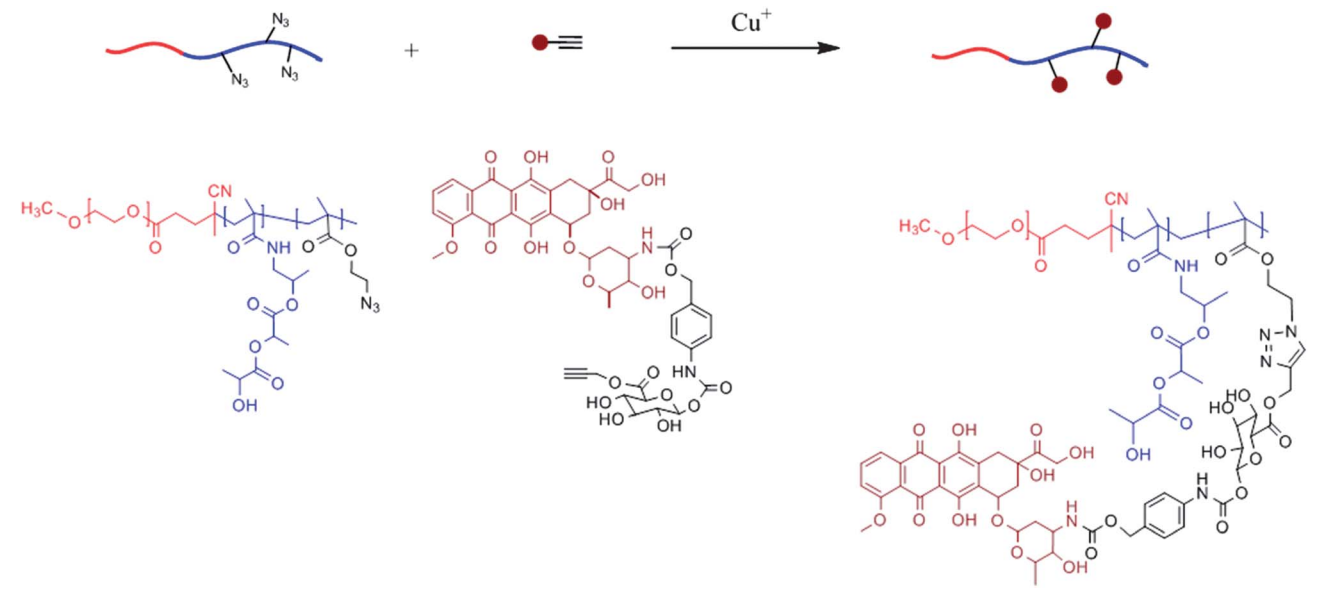

Fig. 2 Schematic representation of the azide–alkyne click-coupling of the mPEG-*b*-p(HPMAmLac$_2$-*co*-AzEMA) polymer with DOX-propGA3.

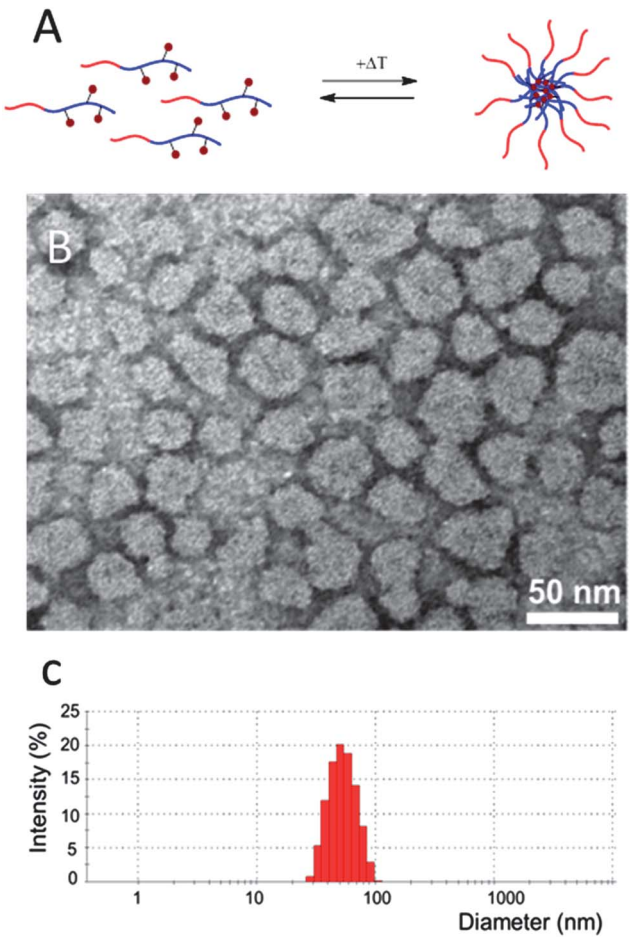

Fig. 3 Schematic representation of the formation of micelles upon rapid heating of prodrug-containing block copolymers (A). TEM observation (B) and hydrodynamic size distribution of DOX-GA3-containing PEG-pHPMAm-based polymeric micelles (C).

micelles in the absence of β-glucuronidase, which is in line with the notion that DOX release from liposomes is relatively slow.[45]

As expected from previous studies,[46] the injection of free DOX into A549 tumor-bearing mice slightly slowed down tumor growth (Fig. 6A and D). Without virus co-treatment, similar antitumor efficacy was observed for pg-micelles, which indicates that the micelles accumulate to some extent in tumors *via* EPR (Enhanced Permeation and Retention),[47,48] and are partially activated by endogenous levels of β-glucuronidase within tumors and tumor cells (lysosomes). When combined with control (GLV-1h190) and β-glucuronidase-producing (GLV-1h68) vaccinia viruses, the pg-micelles turned out to be more efficient than the free drug. It should be taken into account in this regard, however, that at the viral doses used (5×10^6 pfu), both the control and the enzyme-expressing virus were already highly effective in inhibiting tumor growth: as exemplified in Fig. 6B–D, even in the absence of DOX- or pg-micelle-cotreatment, tumor volumes never exceeded 200%, confirming the strong oncolytic potential of vaccinia viruses.[21–27] Interestingly, when combined with free DOX, the oncolytic activity of GLV-1h190 was somewhat reduced (Fig. 6B), but this seems largely due to one non-responder in this group (Fig. 6D). Conversely, when combined with pg-micelles, there was a tendency toward improved efficacy as compared to viral treatment alone (Fig. 6B and D), which manifested in a complete inhibition of tumor growth (*i.e.* never exceeding 100%; Fig. 6B). As expected, this effect is somewhat more pronounced upon combining the pg-micelles with the β-glucuronidase-producing virus (Fig. 6C and D), resulting in significantly smaller tumor volumes as compared to virus treatment alone ($p < 0.01$; Fig. 6D).

To verify that this enhanced efficacy is due to virus-mediated expression of the enzyme, we also assessed the glucuronidase activity levels in the tumors. As shown in the left panel of Fig. 6E, analysis in PBS (pH 7.4) revealed that the glucuronidase

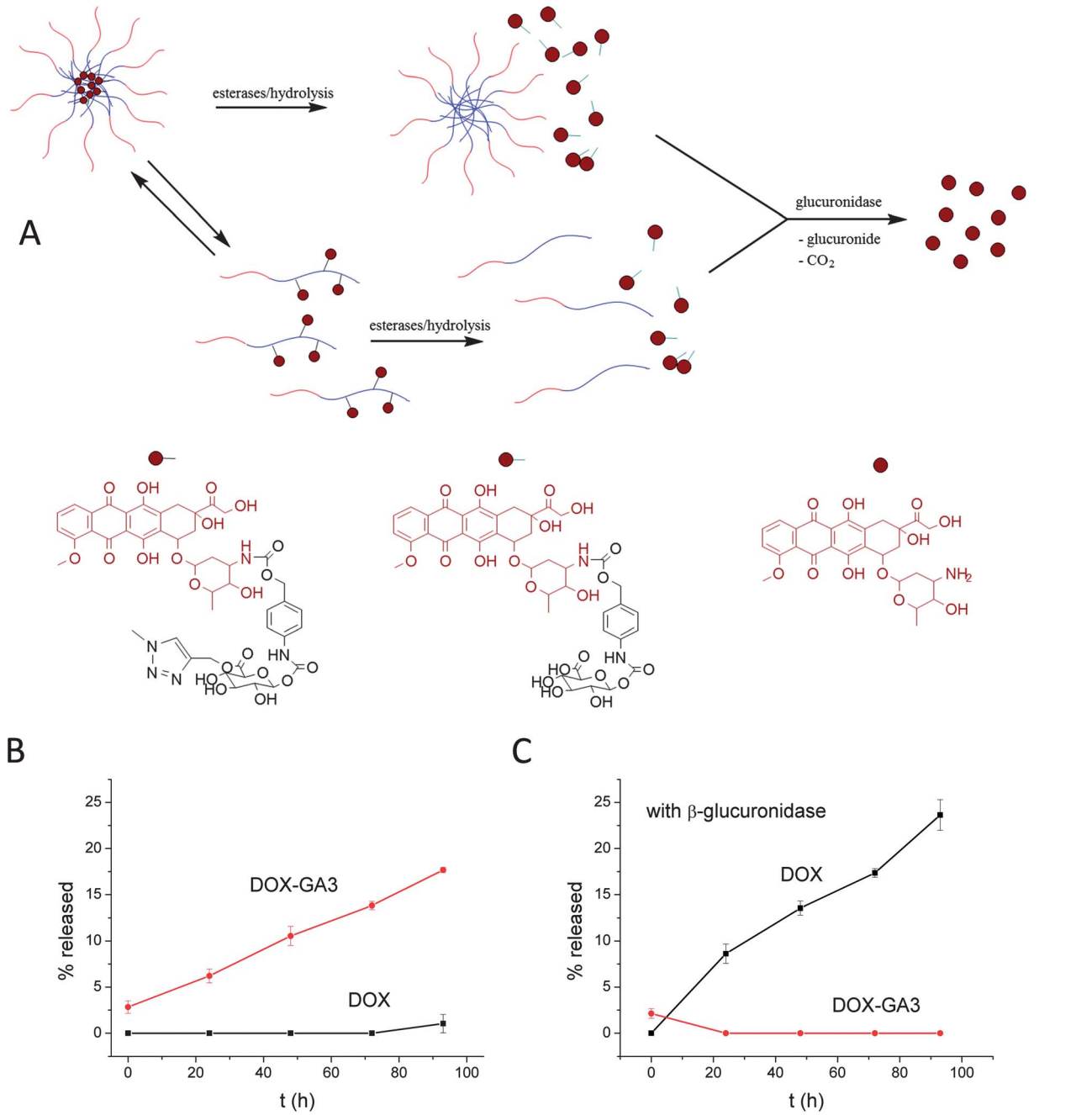

Fig. 4 Schematic representation of the two-step activation of DOX by (1) the hydrolysis of DOX-propGA3 and concomitant release of DOX-GA3 from micelles or free polymer–prodrug conjugates (which exist in a dynamic equilibrium), and (2) enzymatic conversion of DOX-GA3 into free DOX (A). Release profiles of DOX-GA3 and DOX from PEG-pHPMAm-based polymeric micelles in the absence (B) and presence (C) of β-glucuronidase.

activity in GLV-1h68-treated tumors was more than 30-fold higher than in GLV-1h190- and PBS-treated tumors. This confirms successful tumor colonization by GLV-1h68 and efficient production of the enzyme. To discriminate between the GLV-1h68-mediated production of bacterial β-glucuronidase and the release of human β-glucuronidase from A549 cells upon (virus-induced) tumor necrosis, enzyme activity levels were also evaluated at pH 4.5. The right panel in Fig. 6E clearly demonstrates in this regard that the high enzyme activity observed at pH 7.4 is caused by virus-mediated enzyme production (since bacterial β-glucuronidase is more active at neutral than at acidic pH).[49] Under control conditions, on the other hand, *i.e.* upon PBS and GLV-1h190 treatment, the levels of enzyme activity were higher at acidic than at neutral pH (note that human β-glucuronidase has a pH-optimum at 4.8).[49] The fact that enzyme activity at pH 4.5 was higher in GLV-1h190-treated than in PBS-treated animals (right panel of Fig. 6E) explains, at least partially, why pg-micelles were also effective upon treatment

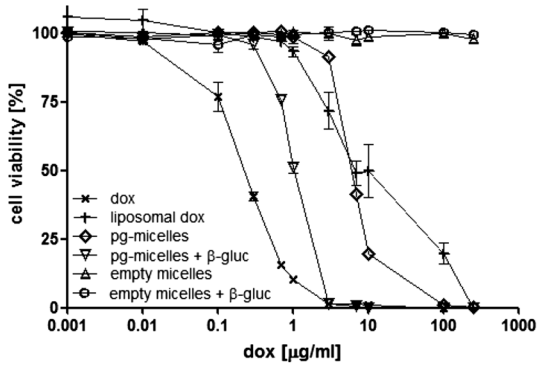

Fig. 5 *In vitro* efficacy of free doxorubicin (DOX), liposomal doxorubicin, empty micelles and doxorubicin-prodrug-containing micelles (pg-micelles) in the presence and absence of β-glucuronidase in A549 human NSCLC cells. Concentrations are plotted as doxorubicin-equivalent concentrations. Empty micelles were used at the same polymer concentrations as those of pg-micelles, ranging from 0.034 to 8600 μg mL^{-1}.

with control viruses (Fig. 6B), likely causing tumor necrosis and thereby resulting in the release of human β-glucuronidase from A549 cells. The observation that the overall levels of enzyme activity, both at pH 7.4 and 4.5, are higher upon GLV-1h68-treatment than upon GLV-1h190- and PBS-treatment is in line with the notion that the combination of GLV-1h68 with pg-micelles appeared to be the most efficient treatment for inhibiting tumor growth (Fig. 6D). Regarding the higher activity of bacterial β-glucuronidase at pH 7.4, it should be noted that since micelles are poorly internalized[50] and virus-encoded β-glucuronidase is released from the tumor cells upon tumor cell lysis,[40] it is expected that part of the prodrug is activated in the extracellular space having a pH close to neutral.

In summary, we here provide proof-of-principle for combining DOX-prodrug-loaded polymeric micelles with standard and β-glucuronidase-producing oncolytic vaccinia viruses, resulting in significantly improved tumor growth inhibition as compared to virotherapy alone. Even though further optimization of the

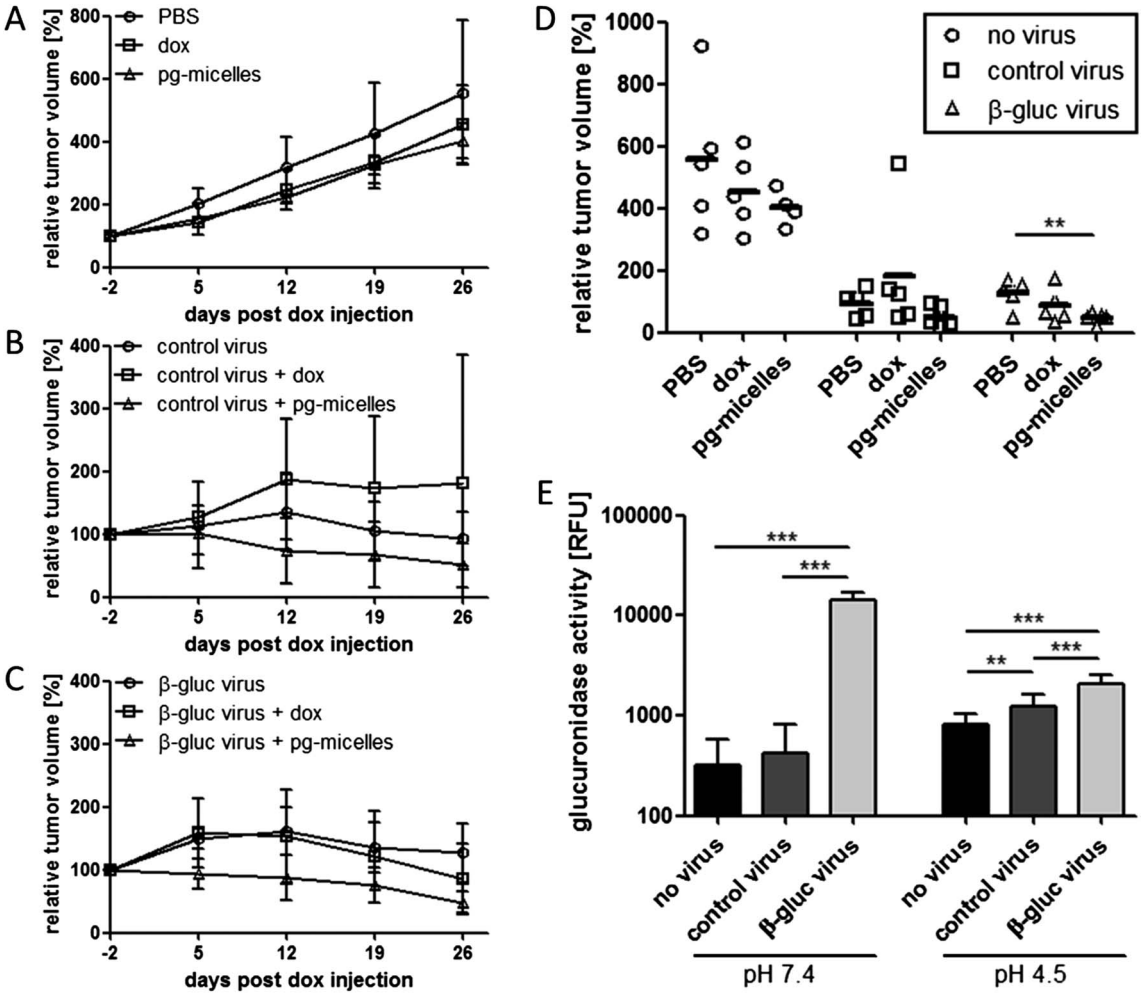

Fig. 6 *In vivo* efficacy of doxorubicin-prodrug-loaded PEG-pHPMAm-based micelles and free doxorubicin alone (A), and in combination with control (B) and β-glucuronidase-producing oncolytic vaccinia viruses (C), in nude mice bearing A549 NSCLC xenograft tumors. Individual relative tumor volumes at the last day of follow-up (day 26), showing significantly improved efficacy upon combining pg-micelles with β-glucuronidase-producing viruses (D). β-Glucuronidase activity levels determined at pH 7.4 and pH 4.5 in lysates from tumors treated with PBS, control virus, and β-glucuronidase-producing virus (E). ** indicates $p < 0.01$ and *** indicates $p < 0.005$.

timing and dosing of virotherapy and tumor-targeted drug delivery is necessary, these findings demonstrate the potential of combined viro–nano-therapy.

Conclusions

A doxorubicin-glucuronide (DOX-propGA3) prodrug has been covalently coupled, *via* click chemistry, to mPEG-*b*-p(HPMAm-Lac_2-*co*-AzEMA) thermosensitive block copolymers, which upon rapid heating in aqueous solution form micelles with a size of ~50 nm and with low polydispersity. The enzyme-responsive activation of DOX was demonstrated *in vitro* in A549 cells in the presence of β-glucuronidase, which is expressed in lysosomes and in necrotic tumor areas. As compared to the free drug, in combination with oncolytic vaccinia viruses, prodrug-loaded micelles led to a complete inhibition of tumor growth, and were significantly more effective than treatment with the viruses alone. These proof-of-principle findings indicate that the combination of tumor-targeted drug delivery with oncolytic virotherapy holds significant potential.

Acknowledgements

This work was financially supported by the European Union (FP7 Marie Curie Intra-European Fellowship for Career Development, project NanoSmart, to ERH; and FP6 MediTrans, to GS), by the European Research Council (Starting Grant 309495, NeoNaNo, to TL) and by a graduate stipend from the University of Würzburg *via* a Research Service Grant awarded by Genelux Corporation (to MH). Teva Pharmachemie has financially supported the synthesis of the prodrug DOX-propGA3. The authors furthermore thank Terry Trevino for assistance in cell culture. JS and AAS are employees and shareholders of Genelux Corporation.

References

1 M. E. Davis, Z. Chen and D. M. Shin, *Nat. Rev. Drug Discovery*, 2008, **7**, 771–782.
2 R. Duncan, *Nat. Rev. Cancer*, 2006, **6**, 688–701.
3 C. Oerlemans, W. Bult, M. Bos, G. Storm, J. F. W. Nijsen and W. E. Hennink, *Pharm. Res.*, 2010, **27**, 2569–2589.
4 T. Lammers, F. Kiessling, W. E. Hennink and G. Storm, *J. Controlled Release*, 2012, **161**, 175–187.
5 C. Deng, Y. Jiang, R. Cheng, F. Meng and Z. Zhong, *Nano Today*, 2012, **7**, 467–480.
6 V. R. Devadasu, V. Bhardwaj and M. Kumar, *Chem. Rev.*, 2013, **113**, 1686–1735.
7 J. Kopecek and P. Kopeckova, *Adv. Drug Delivery Rev.*, 2010, **62**, 122–149.
8 S. Svenson, *Curr. Opin. Solid State Mater. Sci.*, 2012, **16**, 287–294.
9 Y. Shi, M. J. van Steenbergen, E. A. Teunissen, L. Novo, S. Gradmann, M. Baldus, C. F. van Nostrum and W. E. Hennink, *Biomacromolecules*, 2013, **14**, 1826–1837.
10 M. Talelli, S. Oliveira, C. J. F. Rijcken, E. H. E. Pieters, T. Etrych, K. Ulbrich, R. C. F. van Nostrum, G. Storm, W. E. Hennink and T. Lammers, *Biomaterials*, 2013, **34**, 1255–1260.
11 M. Talelli, M. Iman, A. K. Varkouhi, C. J. F. Rijcken, R. M. Schiffelers, T. Etrych, K. Ulbrich, C. F. van Nostrum, T. Lammers, G. Storm and W. E. Hennink, *Biomaterials*, 2010, **31**, 7797–7804.
12 M. Coimbra, C. J. F. Rijcken, M. Stigter, W. E. Hennink, G. Storm and R. M. Schiffelers, *J. Controlled Release*, 2012, **163**, 361–367.
13 B. J. Crielaard, C. J. F. Rijcken, L. Quan, S. van der Wal, I. Altintas, M. van der Pot, J. A. W. Kruijtzer, R. M. J. Liskamp, R. M. Schiffelers, C. F. van Nostrum, W. E. Hennink, D. Wang, T. Lammers and G. Storm, *Angew. Chem., Int. Ed.*, 2012, **51**, 7254–7258.
14 M. Talelli, C. J. F. Rijcken, W. E. Hennink and T. Lammers, *Curr. Opin. Solid State Mater. Sci.*, 2012, **16**, 302–309.
15 K. J. M. Schimmel, D. J. Richel, R. B. A. van den Brink and H. J. Guchelaar, *Cancer Treat. Rev.*, 2004, **30**, 181–191.
16 M. Talelli, K. Morita, C. J. F. Rijcken, R. W. M. Aben, T. Lammers, H. W. Scheeren, C. F. van Nostrum, G. Storm and W. E. Hennink, *Bioconjugate Chem.*, 2011, **22**, 2519–2530.
17 N. G. Beratis, A. Kaperonis, M. I. Eliopoulou, G. Kourounis and V. A. Tzingounis, *J. Cancer Res. Clin. Oncol.*, 2005, **131**, 371–376.
18 H. M. Dodds, P. J. Tobin, C. F. Stewart, P. Cheshire, S. Hanna, P. Houghton and L. P. Rivory, *J. Pharmacol. Exp. Ther.*, 2002, **303**, 649–655.
19 B. Sperker, U. Werner, T. E. Murdter, C. Tekkaya, P. Fritz, R. Wacke, U. Adam, M. Gerken, B. Drewelow and H. K. Kroemer, *Naunyn-Schmiedeberg's Arch. Pharmacol.*, 2000, **362**, 110–115.
20 K. Bosslet, R. Straub, M. Blumrich, J. Czech, M. Gerken, B. Sperker, H. K. Kroemer, J. P. Gesson, M. Koch and C. Monneret, *Cancer Res.*, 1998, **58**, 1195–1201.
21 N. G. Chen and A. A. Szalay, *Future Virol.*, 2010, **5**, 763–784.
22 D. H. Kirn and S. H. Thorne, *Nat. Rev. Cancer*, 2009, **9**, 64–71.
23 K. Guse, V. Cerullo and A. Hemminki, *Expert Opin. Biol. Ther.*, 2011, **11**, 595–608.
24 Y. A. Yu, S. Shabahang, T. M. Timiryasova, Q. Zhang, R. Beltz, I. Gentschev, W. Goebel and A. A. Szalay, *Nat. Biotechnol.*, 2004, **22**, 313–320.
25 J. Stritzker, L. Kirscher, M. Scadeng, N. C. Deliolanis, S. Morscher, P. Symvoulidis, K. Schaefer, Q. Zhang, L. Buckel, M. Hess, U. Donat, W. G. Bradley, V. Ntziachristos and A. A. Szalay, *Proc. Natl. Acad. Sci. U. S. A.*, 2013, **110**, 3316–3320.
26 N. Chen, Q. Zhang, Y. A. Yu, J. Stritzker, P. Brader, A. Schirbel, S. Samnick, I. Serganova, R. Blasberg, Y. Fong and A. A. Szalay, *Mol. Med.*, 2009, **15**, 144–151.
27 D. Haddad, N. G. Chen, Q. Zhang, C. H. Chen, Y. A. Yu, L. Gonzalez, S. G. Carpenter, J. Carson, J. Au, A. Mittra, M. Gonen, P. B. Zanzonico, Y. Fong and A. A. Szalay, *J. Transl. Med.*, 2011, **9**, 36.
28 S. S. Kelkar and T. M. Reineke, *Bioconjugate Chem.*, 2011, **22**, 1879–1903.

29 T. Lammers, S. Aime, W. E. Hennink, G. Storm and F. Kiessling, *Acc. Chem. Res.*, 2011, **44**, 1029–1038.
30 J. J. Rojas and S. H. Thorne, *Theranostics*, 2012, **2**, 363–373.
31 L. Buckel, S. J. Advani, A. Frentzen, Q. Zhang, Y. A. Yu, N. G. Chen, K. Ehrig, J. Stritzker, A. J. Mundt and A. A. Szalay, *Int. J. Cancer*, 2013, **133**, 2989–2999.
32 S. J. Advani, L. Buckel, N. G. Chen, D. J. Scanderbeg, U. Geissinger, Q. Zhang, Y. A. Yu, R. J. Aguilar, A. J. Mundt and A. A. Szalay, *Clin. Cancer Res.*, 2012, **18**, 2579–2590.
33 Y. A. Yu, C. Galanis, Y. Woo, N. Chen, Q. Zhang, Y. Fong and A. A. Szalay, *Mol. Cancer Ther.*, 2009, **8**, 141–151.
34 A. Frentzen, Y. A. Yu, N. Chen, Q. Zhang, S. Weibel, V. Raab and A. A. Szalay, *Proc. Natl. Acad. Sci. U. S. A.*, 2009, **106**, 12915–12920.
35 C. M. Seubert, J. Stritzker, M. Hess, U. Donat, J. B. Sturm, N. Chen, J. M. von Hof, B. Krewer, L. F. Tietze, I. Gentschev and A. A. Szalay, *Cancer Gene Ther.*, 2011, **18**, 42–52.
36 M. de Graaf, E. Boven, H. W. Scheeren, H. J. Haisma and H. M. Pinedo, *Curr. Pharm. Des.*, 2002, **8**, 1391–1403.
37 D. Neradovic, O. Soga, C. F. Van Nostrum and W. E. Hennink, *Biomaterials*, 2004, **25**, 2409–2418.
38 Q. Zhang, Y. A. Yu, E. Wang, N. Chen, R. L. Danner, P. J. Munson, F. M. Marincola and A. A. Szalay, *Cancer Res.*, 2007, **67**, 10038–10046.
39 H. Wang, N. G. Chen, B. R. Minev and A. A. Szalay, *J. Transl. Med.*, 2012, **10**, 167.
40 M. Hess, J. Stritzker, B. Hartl, J. B. Sturm, I. Gentschev and A. A. Szalay, *J. Transl. Med.*, 2011, **9**, 172.
41 R. W. M. Aben, H. W. Scheeren, J. J. Cornelissen, M. Lamberuts, D. de Vos, H. J. Haisma, EP Application, EP2098533 A1, 2009.
42 M. van Dijk, D. T. S. Rijkers, R. M. J. Liskamp, C. F. van Nostrum and W. E. Hennink, *Bioconjugate Chem.*, 2009, **20**, 2001–2016.
43 C. J. Rijcken, C. J. Snel, R. M. Schiffelers, C. F. van Nostrum and W. E. Hennink, *Biomaterials*, 2007, **28**, 5581–5593.
44 P. H. J. Houba, E. Boven, I. H. van der Meulen-Muileman, R. G. G. Leenders, J. W. Scheeren, H. M. Pinedo and H. J. Haisma, *Int. J. Cancer*, 2001, **91**, 550–554.
45 Y. Barenholz, *J. Controlled Release*, 2012, **160**, 117–134.
46 L. Kraus-Berthier, M. Jan, N. Guilbaud, M. Naze, A. Pierre and G. Atassi, *Clin. Cancer Res.*, 2000, **6**, 297–304.
47 H. Maeda, J. Wu, T. Sawa, Y. Matsumura and K. Hori, *J. Controlled Release*, 2000, **65**, 271–284.
48 V. Torchilin, *Adv. Drug Delivery Rev.*, 2011, **63**, 131–135.
49 T. V. Zenser, V. M. Lakshmi and B. B. Davis, *Drug Metab. Dispos.*, 1999, **27**, 1064–1067.
50 M. Talelli, M. Iman, C. J. F. Rijcken, C. F. van Nostrum and W. E. Hennink, *J. Controlled Release*, 2010, **148**, e121–e122.